

# Sizes of Lightest Glueballs in SU(3) Lattice Gauge Theory

Mushtaq Loan

*Department of Physics, Zhongshan (Sun Yat-Sen) University, Guangzhou 510275, China  
School of Physics, The University of New South Wales, Sydney, NSW 2052, Australia*

Yi Ying

*Department of Physics, Chong Qing University, Chong Qing 400030, China*

(Dated: February 8, 2020)

Standard Monte Carlo simulations have been performed on improved lattices to measure the wave functions and the sizes of the scalar and tensor glueballs at four lattice spacings in the range  $a = 0.05 - 0.145$  fm. Systematic errors from discretization and finite volume are studied. Our results in the continuum limit show that the size of the tensor state is approximately two times as large as that of the scalar glueball.

PACS numbers: 11.15.Ha, 12.38.Gc, 11.15.Me

## I. INTRODUCTION

State of art lattice calculations have produced very accurate spectroscopic information of the low-lying hadrons [1, 2] and glueballs [3, 4, 5, 6, 7]. These calculations show that lowest-lying scalar, tensor and axial vector glueballs lie in the mass region of 1-2.5 GeV. While there is a long history of hadron and glueball mass calculations in lattice QCD, progress in determining their wave functions has not been so rapid. The spectrum of pure gauge QCD cannot be directly compared to experiment, it is important to pin it down because so little is known about glueball properties. The mixing of glueballs with  $q\bar{q}$  mesons due to the presence of the light dynamical makes it difficult in distinguishing them from ordinary mesons both in full lattice QCD as well as in the experiments [8]. Enormous efforts have been and are being made in pursuit of the glueballs and their properties [9]. Accurate lattice calculations of their size, matrix elements and form factors would help considerably their experimental identification.

Glueball wave functions and sizes have been studied in the past [10, 11, 12, 13] but much of the early work contains uncontrolled systematic errors, most notably from discretization effects. On the other hand, the calculations using operator overlaps obtained from variational optimization for improved lattice gauge action show that the scalar and tensor glueballs were of typical hadronic dimensions. A straightforward procedure to address the controversy of glueball size is to measure the glueball wave function, much the same way as the meson and baryon wave functions were measured.

Although Ref. [10] has produced interesting results, the approach suffers from a basic problem: the observables are calculated from lattice version of the 2-glue operator, which risks a mixture of glueball states with flux state<sup>1</sup>. Also the results were of limited interest because

of their manifest dependence on the gauge chosen. In this study we take a more direct approach to the problem; instead of fixing a gauge or a path for the gluons, we measure the correlation functions from spatially connected Wilson loops which, being the expectation values of closed-loop paths, are gauge invariant. The procedure has been used in the measurement of wave functions of the scalar and tensor glueballs in the lattice Monte Carlo calculation for 3-dimensional U(1) theory [14]. This approach has the advantage that the disentangling of the glueball and torelon is usually taken care of automatically by the choice of Wilson or Polyakov loops. This means that glueball operators cannot create a single torelon state, but the creation of torelon-antitorelon pairs is possible.

In this paper, we demonstrate the efficiency of our method to calculate SU(3) glueball wave functions using improved action. Since we want to explore the nature of the wave function, we focus on the sizes and masses of two of the lighter SU(3) glueball states, the scalar and the tensor. To avoid the mixing effects, we adopt a quenched lattice QCD as a necessary first step before attempting to include the effect of dynamical quarks in the future. It is worth mentioning here that quenched lattice QCD reproduces well the important nonperturbative quantities as well as masses of hadrons, mesons, and baryons. The remaining contents of this paper are organized as follows. In Sec. II we give a prescription how to calculate the glueball wave function and size based on the information from glueball correlators with the smearing method. We present and discuss our results in Sec. III. We close this section with a comparison of our results with the related QCD results. Our concluding remarks are given in Sec. IV.

---

<sup>1</sup> The link-link operator used sums up a large number of loops;

some of these loops have a zero winding number and project on glueballs - others have non-zero winding number and project on flux states also called torelons.

## II. WAVE FUNCTIONS OF GLUEBALLS

The lattice observables are measured as follows. First, we calculated the lattice operator

$$\Phi_i(\vec{r}, t) = \sum_x [\phi_i(\vec{x}, t) + \phi_i(\vec{x} + \vec{r}, t)], \quad (1)$$

where  $\phi$  is the plaquette operator and  $\Phi$  is the two-plaquette or two-loop component of the glueball wave function. The summation over  $x$  is performed for the zero-momentum projection. The  $r$  dependence will be reflected in the length of links required to close the loops.

Given a pair of orbit- and spin- quantum numbers  $L$  and  $S$  for the desired glueball, one can construct operators  $W(|\vec{r}|, t)$  with  $J = 0, 1, 2$ ,  $P = \pm$ , and  $C = \pm$  from suitable linear combinations of rotation, parity inversions and real or imaginary parts of the operators involved in  $\Phi$ . In this study we only consider  $S = L = 0$  and  $S = 2$ ,  $L = 0$ . The two lattice observables measured are therefore

$$W_0(|\vec{r}|, t) = \sum_r [\Phi_{12} + \Phi_{13} + \Phi_{23}], \quad (2)$$

$$W_2(|\vec{r}|, t) = \sum_r [2\Phi_{12} - \Phi_{23} - \Phi_{13}]. \quad (3)$$

Using the glueball operators  $W$ , we consider the correlator of the glueball as

$$C(\vec{r}, t) = \langle W^\dagger(\vec{r}, t)W(\vec{r}, 0) \rangle, \quad (4)$$

where the vacuum expectation value needs to be subtracted for the  $0^{++}$  glueball. The source can be held fixed while the sink takes on the  $r$  dependence. This proves to be helpful in maintaining a good signal. In general, to measure the ground-state mass from the correlator, one seeks for the region where the overlap with lowest state is maximum and contributions from excited states almost die out. In principle, such a region always exists for large Euclidean time  $t$  in the zero-temperature case. However, in practice, it is difficult to use such large  $t$  in lattice QCD Monte Carlo calculations, since correlator decreases exponentially with  $t$  and becomes so small for large  $t$  that is comparable to its statistical errors. Hence, for the ground-state mass measurement, it is important that the ground-state overlap should be sufficiently large. This amounts to a discrete search among wave functions. In the case of glueballs in quenched SU(3) lattice QCD, the overlap of the operators given in Eqs. (2) and (3) are quite small as long as they are constructed from the simple plaquette operators. This small overlap originates from the fact that the plaquette operator has a smaller “size” of  $O(a)$  than the physical size of the glueball [15]. To improve the glueball operator, for enhancing the ground-state contribution, we exploit the APE link smearing techniques [15, 16] to generate extended operators that have approximately the same size as the physical size of the glueball. The smearing

procedure is implemented by the iterative replacement of the original spatial link variable by a smeared link. As for the smearing parameters, which play an important role in extracting the ground-state contribution, we used a smearing fraction of  $\alpha = 0.5$  and smearing number  $N_{\text{smr}} = 15$  in the present calculation. The optimum smearing is determined by examining the ratio

$$C(r, t+1)/C(r, t)$$

which should be close to unity for good ground state dominance. In fact, in the range as  $4 \leq N_{\text{smr}} \leq 11$ , the above ratio is almost unchanged. For our measurements, with  $\alpha = 0.5$  fixed, a typical value which proved to be sufficient for most cases was  $N_{\text{smr}} = 4$  (although the results are almost the same as those with  $N_{\text{smr}} = 11$ ). For fixed  $\alpha$ ,  $N_{\text{smr}}$  plays the role of extending the size of the smeared operator and hence can give the rough estimate of the physical size of the glueball.

A second pass was made to measure the optimized correlation matrices

$$C_{ij}(t) = \langle W(r_i, t)W(r_j, 0) \rangle - \langle W(r_i) \rangle \langle W(r_j) \rangle. \quad (5)$$

Let  $\psi^{(k)}$  be the radial wave function of the  $k$ -th eigenstate of the transfer matrix, then

$$C_{ij}(t) = \sum_k \alpha_k \psi^{(k)}(r_i) \psi^{(k)}(r_j) e^{-m_k t}. \quad (6)$$

The glueball masses and the wave functions are extracted from the Monte Carlo average of  $C_{ij}(t)$  by diagonalizing the correlation matrices  $C(t)$  for successive times  $t$ :

$$C(t) = \tilde{R}(t)D(t)R(t), \quad (7)$$

where  $D$  is a diagonal matrix of the eigenvalues and  $R$  a rotation matrix whose columns are the eigenvectors of  $C$ . Each eigenvector of  $C$  matches an eigenstate  $\psi^{(k)}(r)$  of the complete transfer matrix.

In order to investigate the size of the glueball, the Bethe-Salpeter amplitude provides a convenient tool. In the nonrelativistic limit, it is expected to reduce to the glueball wave function in the first-quantized picture. This property can be exploited to estimate the size of the glueball [10]. Similar to the case for mesons, the wave function is expected to decrease exponentially with the separation  $r$  and is therefore fitted with the simple form

$$\psi(r) \equiv e^{-r/r_0} \quad (8)$$

to determine the effective radius  $r_0$ .

The signal in the connected 2-point correlator  $C(t)$  for all observables does not last long enough to make to an exponential falloff. The data is therefore presented in terms of the effective mass read off directly from the largest eigenvalue corresponding to the lowest energy

$$m_{\text{eff}} = \log \left[ \frac{\lambda_0(r=0, t=1)}{\lambda_0(r=0, t=2)} \right]. \quad (9)$$

However, to ensure the validity of our results, we make checks using

$$m'_{eff} = \left[ \frac{\lambda_0(t-1) - \lambda_0(t)}{\lambda_0(t) - \lambda_0(t+1)} \right]. \quad (10)$$

### III. SIMULATIONS RESULTS AND DISCUSSION

An ensemble of gauge configurations are generated by a combination of the Cabibbo-Marinari (CM) algorithm and the overrelaxed method. Configurations were given a hot start and then 100 compound sweeps (we define one compound sweep as one CM update followed five overrelaxation sweeps) in order to equilibrate. After thermalization, configurations are stored every 50 compound sweeps for 750 configurations. Measurements made on the stored configurations are binned into 10 blocks with each block containing an average of 75 measurements. The mean and the final errors are obtained using single-elimination jackknife method with each bin regarded as an independent data point. Four sets of measurements were taken to check the scaling of our results at  $\beta = 2.0, 2.25, 2.5$  and  $2.75$  on  $16^3 \times 16$  lattice. Some finite-size consistency checks are done on a  $12^3 \times 12$  lattice. Even though the lattice is relatively coarse, we can safely argue that there are no large discretization errors after the implementation of improved gauge and fermion actions.

The glueball correlation function for the  $0^{++}$  channel against  $t$  at  $\beta = 2.5$  is shown in Fig. 1. The correlation function shows the expected exponential behaviour against Euclidean time  $t$  for small  $r$  values. Concerning the determination of the tensor glueball we observe that signal for  $E^{++}$  channel is better than for  $T_2^{++}$  and errors on the effective mass are reasonable. For this reason we choose to use  $E$  of the tensor at finite lattice spacing. At  $\beta = 2.0$  the signal does not persist long enough to demonstrate convergence to the asymptotic value, we quote results for time separations  $t = 1$  and  $2$ . We found that evaluations of Eqs. (9) and (10) yield very consistent results in all case analyzed here. The best estimates for masses from our long runs are collected in Table I.

We extract the wave functions at time-separations  $t = 1$ . Little variation in the eigenvectors of  $C(t)$ , at  $t = 1$  and  $2$ , was found which suggests that there is no mixing with the states of distinct masses. Typical plots of the wave functions, normalized to unity at the origin, for the scalar and tensor glueballs, at  $\beta = 2.25, 2.5$  and  $2.75$  are shown in Figs. 2 and 3 respectively. For guiding the eyes the Monte Carlo points of the same  $\beta$ -value are connected with straight lines. The scalar wave function shows the expected behaviour and remains positive for all the  $\beta$  values analyzed here.

The tensor wave function shows the expected flatness and is much more extended than the scalar as one moves towards higher  $\beta$  values. This would imply that tensor is

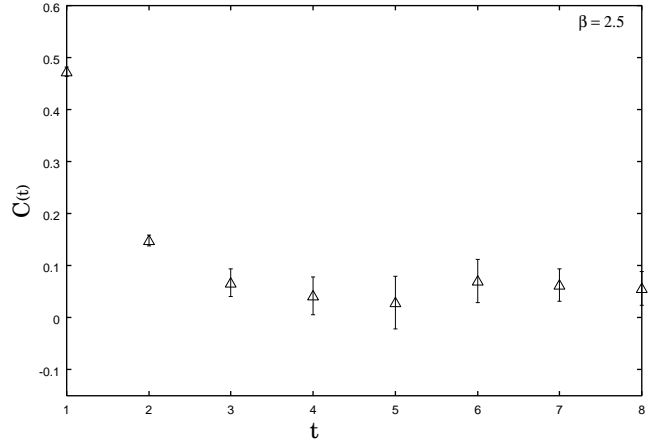


FIG. 1: Correlation function for the scalar glueball at  $\beta = 2.5$  on  $16^4$  lattice.

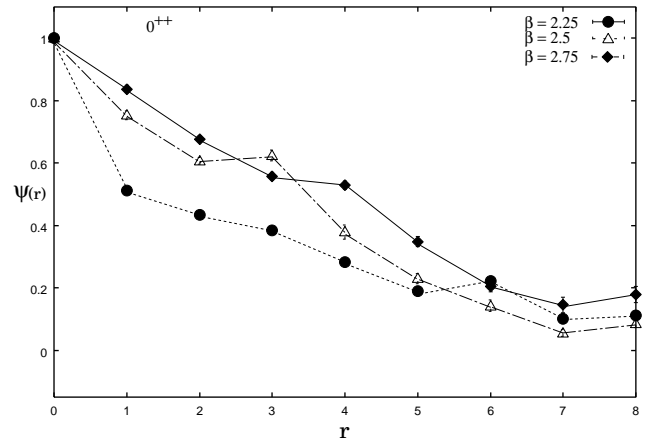


FIG. 2: SU(3) Scalar glueball wave functions measured on  $16^4$  lattice for various values of  $\beta$ .

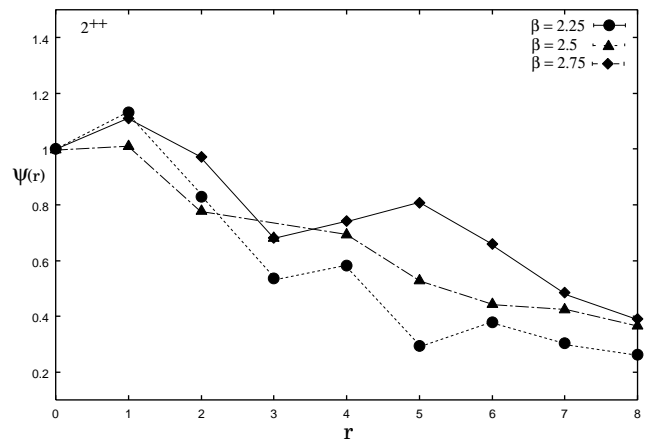


FIG. 3: Wave functions of tensor glueball measured on  $16^4$  lattice at  $\beta = 2.25, 2.5$  and  $2.75$ .

therefore more sensitive to the finite-size effects, which is very visible in the distortion of the wave function for large

$r$  at  $\beta = 2.75$ . Naively we would expect that the spatial size at which we begin to encounter large finite size effects to be related to the size of the glueball. The optimization analysis at  $t = 1/0$  found the  $4 \times 4$  and  $5 \times 5$  loops have a better overlap with glueball. This would suggest that the glueballs have a size of  $\sim 4a - 5a$ . The smaller loops showed a weak signal with a slow convergence with  $N_{\text{SMR}}$ . This is consistent with the findings of APE when using  $1 \times 1$  loop as template.

The size of the glueball is actually a nontrivial quantity. Although the charge radius of the glueball can be formally defined, its electric charges are carried by the quarks and antiquarks, which play only of secondary roles in describing the glueball state in the idealized limit, since the glueball by its nature does not contain any valence contents of quarks (antiquarks). In principle, one could use Eq. (8) to extract the effective radius, but because of the distortion of the wave function at large  $r$  the results will differ by fit-analysis of the above form. Even after the ground-state enhancement is performed, the complete elimination of all the contributions of the excited states is impossible, especially near  $r \sim 0$ . It follows that Eq. (8) holds only in the limited interval, which does not include the vicinity of  $r \sim 0$ . Hence, for the accurate measurement of the effective radius, we need to find the appropriate fit range. To this end, we examine the effective-radius plot and the ratio

$$\log \left[ \frac{\psi(r)}{\psi(r+1)} \right]$$

for a given  $\psi(r)/\psi(r+1)$  at each fixed  $r$ . In Fig. 4 we plot the effective radius  $r_0$  against  $r$  associated with Figs. 2 and 3 at  $\beta = 2.75$ . In Fig. 4 shows a nontrivial  $r$  dependence, in the neighborhood of  $r \sim 0$ , in the effective radius of the tensor state. However, at large  $r$ , we see that there appears a region where  $r_0$  takes almost a constant value, thus we expect that  $r_0$  consists of nearly a single spectral component, and, hence can properly represent the effective radius. The estimates of the sizes, in the lattice units, at various  $\beta$  values are shown in Table II.

In order to ascertain the finite-size effect on our measurements, we performed extra simulations for  $\beta = 2.5$  and  $2.75$  using lattice of spatial extent  $L = 12$ . The results from this spatial extension for glueball masses in terms of lattice units are given in Tables I and II respectively. Note that the results from the smaller volume differ very little from those from  $16^3$  lattice, indicating that systematic errors in these results from finite volume are negligible. We also find that our estimates for the size of glueballs are consistent with no large finite volume dependence at  $\beta = 2.75$ . Given that we use the larger lattice size to extract our results, the factor clouding the issue that the glueball signal may be contaminated by a torelon-antitorelon pair is disregarded from consideration, since no mass reductions of sufficient magnitudes were found as the lattice volume was reduced (see Table I). This would suggest that none of our states could be

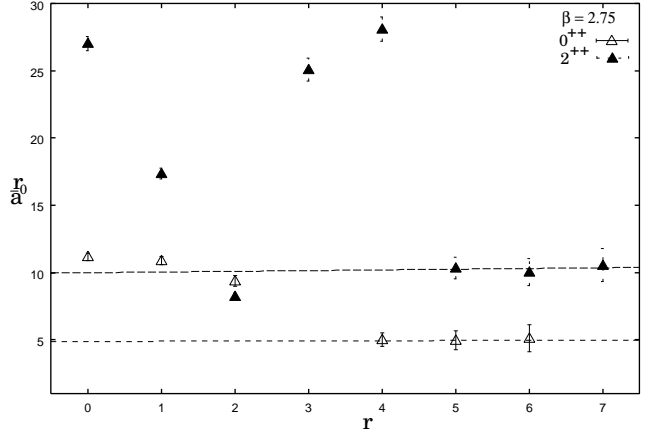


FIG. 4: The effective radius plot for the scalar and tensor glueball states at  $\beta = 2.75$ . The dashed horizontal lines indicate the plateau values.

interpreted as a torelon pair.

TABLE I: Scalar and tensor glueball energy estimates in lattice units for spatial extensions,  $L = 12$  and  $L = 16$ . Also are shown our estimates of the rho mass at physical point on  $L=16$  lattice.

| $\beta/L$ | Mass          |          |               |           |                     |          |
|-----------|---------------|----------|---------------|-----------|---------------------|----------|
|           | $am_{0^{++}}$ |          | $am_{2^{++}}$ |           | $am_\rho(\kappa_c)$ |          |
|           | 12            | 16       | 12            | 16        | 16                  |          |
| 2.0       |               | 0.801(5) |               |           | 1.42(2)             | 0.563(3) |
| 2.25      |               | 0.58(1)  |               |           | 1.07(2)             | 0.391(4) |
| 2.5       | 0.52(2)       | 0.527(3) | 0.82(2)       | 0.824(16) | 0.288(4)            |          |
| 2.75      | 0.43(2)       | 0.443(4) | 0.64(2)       | 0.659(14) | 0.227(4)            |          |

TABLE II: Effective radii of scalar and tensor glueballs in lattice units for two spatial extensions,  $L = 12$  and  $L = 16$ .

| $\beta/L$ | Size             |         |                  |            |
|-----------|------------------|---------|------------------|------------|
|           | $r_0^{0^{++}}/a$ |         | $r_0^{2^{++}}/a$ |            |
|           | 12               | 16      | 12               | 16         |
| 2.0       |                  | 1.37(7) |                  | 3.08(14)   |
| 2.25      |                  | 2.9(1)  |                  | 5.5(5)     |
| 2.5       | 4.1(1)           | 4.23(4) | 7.6(8)           | 7.5(6)     |
| 2.75      | 4.8(2)           | 4.77(6) | 10.0(1.3)        | 9.95(1.24) |

To convert scalar and tensor glueball sizes and masses to physical units and extrapolate to the continuum limit we first need an estimate of lattice spacing. One natural choice for this conversion factor is the rho mass  $m_\rho a$ . This can be done by extrapolating the  $\rho$  mass to the phys-

ical quark mass<sup>2</sup>. Using tadpole-improved clover fermion action we estimate  $1/\kappa_c = 6.362(3)$  from the extrapolating square pion masses from the largest five  $\kappa$  values at  $\beta = 2.5$ . We find that a linear fit of  $m_\pi^2$  in  $1/\kappa$  does work well for rest of the coupling values analyzed here. Linearly extrapolating the  $\rho$  mass to  $\kappa_c$ , we find  $am_\rho(\kappa_c) = 0.288(4)$  or  $a^{-1} = 2.66(5)$  GeV, where the error is a jackknife estimate. The lattice spacings at other  $\beta$  values are listed in Table III.

Another possible error that might effect the simulation results comes from the scaling violation for our action. Expecting that dominant part of scaling violation errors from the gauge and light quark sectors are largely eliminated by tadpole improvement, we extrapolate the results at finite  $a$  to the continuum limit  $a \rightarrow 0$ . In practice it is often difficult to quantify the magnitude of systematic errors arising from this origin. Here we adopt an  $a^2$ - linear extrapolation for the continuum limit, because the leading order scaling violation is always  $O(a_s^2 \Lambda_{\text{QCD}} m_q)$ . We also perform an  $a$ -linear extrapolation to estimate systematic errors. In practice we use the results at three finest lattice spacings for the continuum extrapolation, excluding results at  $\beta = 2.0$ , which appear to have large discretization errors as expected from the naive order estimate.

TABLE III: The lightest SU(3) glueball energy and size estimates in terms of  $\rho$  mass.

| $\beta$ | $a(\text{fm})$ | $m_{0^{++}}/m_\rho$ | $m_{2^{++}}/m_\rho$ | $r_0^{0^{++}} m_\rho$ | $r_0^{2^{++}} m_\rho$ |
|---------|----------------|---------------------|---------------------|-----------------------|-----------------------|
| 2.0     | 0.1444(6)      | 1.422(8)            | 2.53(4)             | 0.77(5)               | 1.73(4)               |
| 2.25    | 0.100(2)       | 1.50(2)             | 2.76(6)             | 1.15(4)               | 2.17(9)               |
| 2.5     | 0.073(3)       | 1.83(3)             | 2.86(4)             | 1.18(3)               | 2.2(1)                |
| 2.75    | 0.058(6)       | 1.95(4)             | 2.87(5)             | 1.12(5)               | 2.26(14)              |

Performing such extrapolations for mass and size we adopt the choice which shows the smoothest scaling behaviour for the final value, and use others to estimate the systematic errors.

Fig. 5 collects and displays our results for the scalar and tensor glueball radii in terms of  $m_\rho$ . Linear extrapolations in  $a^2$  yield better fits, with confidence level of 80 – 85%, and a continuum limits of  $1.14 \pm 0.08$  and  $2.27 \pm 0.03$  for the scalar and tensor states, respectively.

We notice that the product  $r_0^{0,2} m_\rho$  varies only slightly over the fitting range. The three non-zero lattice spacing values of the product are within 0.02 - 0.04 and 0.01 - 0.09 standard deviations of the extrapolated zero lattice spacing result for the scalar and tensor state, respectively. This will make for unambiguous and accurate continuum extrapolations. Fig. 6 shows the dimension-

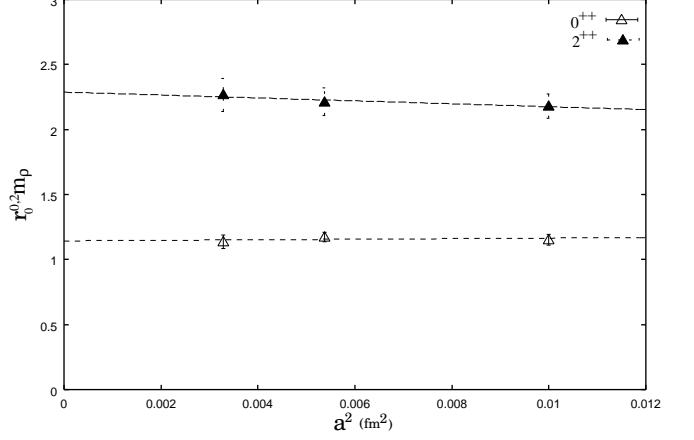


FIG. 5: Continuum limit extrapolation of glue radii in terms of  $\rho$  mass. The dashed curves are the best fits to the simulation results over the range  $0.0033 \leq a^2 \leq 0.01$ .

less ratio  $m_{0,2}/m_\rho$  against the square of the lattice spacing. Again, we expect linear fit in  $a^2$  to provide the most reliable extrapolation to the  $a \rightarrow 0$  limit. Linear extrapolations to the continuum limit yield the scalar estimate of  $2.19 \pm 0.06$  and the tensor result of  $2.95 \pm 0.12$ . In contrast to the tensor, the scalar glueball mass shows significant finite-spacing errors. The continuum limit results obtained, in terms rho mass, are summarized in the Table IV.

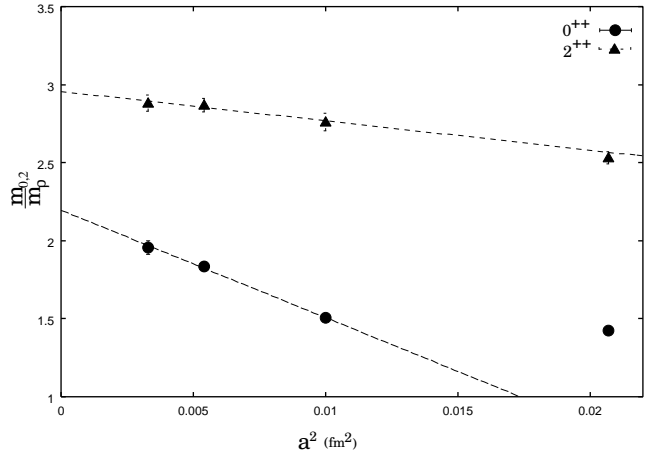


FIG. 6: Continuum limit extrapolation of the glue energy estimates in terms of  $\rho$  mass. The curves are linear fits to the data over the range  $0.0033 \leq a^2 \leq 0.01$ .

To obtain the masses and the radii in units of MeV and fm, we use the experimental value 768 MeV for  $m_\rho$ . This yields radii of  $0.29 \pm 0.02$  and  $0.58 \pm 0.01$  fm for the scalar and tensor glueball, respectively. Our results show that the scalar glueball has a radius roughly equal to that of a pion [17] and tensor glueball is about two times as large as the scalar glueball. This measure of glueball size finds them to be comparable in extend to other hadrons. The

<sup>2</sup> Vaccarino and Weingarten [4] noted that extrapolating to zero lattice spacing using  $[\Lambda]^{(0)}_{MS^a}$  should give results nearly equivalent to those found using  $m_\rho(a)a$ .

TABLE IV: Continuum limit predictions for the scalar and tensor glueball masses and sizes and their conversion to MeV and fm respectively.

|                       |                     |
|-----------------------|---------------------|
| $m_{0^{++}}/m_\rho$   | $2.19 \pm 0.06$     |
| $m_{2^{++}}/m_\rho$   | $2.95 \pm 0.12$     |
| $r_0^{0^{++}}/m_\rho$ | $1.14 \pm 0.08$     |
| $r_0^{2^{++}}/m_\rho$ | $2.27 \pm 0.03$     |
| $m_{0^{++}}$          | $1680 \pm 46$ MeV   |
| $m_{2^{++}}$          | $2265 \pm 92$ MeV   |
| $r_0^{0^{++}}$        | $0.29 \pm 0.02$ fm  |
| $r_0^{2^{++}}$        | $0.58 \pm 0.007$ fm |

continuum limit glueball mass results in MeV are summarized in Table IV. Our glueball mass results are in good agreement with earlier calculations using improved gauge action [3] as well as with those obtained with the Wilson action [4]. It is encouraging that the results are, within 10–15% errors, independent of the lattice action. We find that our glueball size estimates are consistent with the results reported in Ref. [13] obtained by using Gaussian extension as a characteristic size of the glueball. We believe that our physical glueball sizes are more accurate than those obtained in Ref. [10] which show that the radius of the tensor glueball is three times that of a pion and four times that of a scalar glueball. The predicted zero lattice spacing results are not actually found by extrapolation to the zero lattice spacing, but are instead obtained from calculations at  $\beta$  of 2.2 of glueball effective radius. Assigning a physical value to the lattice spacing  $a$  by setting the string tension to 420 MeV the physical radius is calculated with zero uncertainty, with no accurate representation of the effect of the absence of extrapolation.

#### IV. CONCLUSION

To conclude, we have calculated the SU(3) glueball wave functions using improved gauge and fermion lat-

tice actions. Instead of fixing a gauge or a path for gluons, the correlation function were measured from gauge invariant closed-loop paths. This approach has an advantage over the method used in Ref [10] which risked a mixing of the glueball states with torelons and disentangling of the glueball and torelon was done by hand. The iterative smearing procedure discussed here can be used to give a rough estimate of the physical glueball size in terms of Gaussian extension. Although easy to implement, it does not give detailed information about the glueball wave function. A better approach may be to construct an elaborate smearing procedure that maps onto the wave function in one step (i.e., variational method combined with fuzzing techniques).

Finally we note that our results at the finest lattice spacings seem to scale, thus making for very accurate extrapolations to the continuum limit. It is learned that physical glueball size of the tensor state is about two times as large as that of the scalar glueball. This is consistent with the large finite-size effect for the tensor ( $E^{++}$ ) glueball mass found in previous lattice calculations. A great deal of care should be taken in making direct comparisons with experiment since these values neglect the effects of light quarks and mixings with nearby conventional mesons. We intend to include the effect of the dynamical quarks in our future study.

#### Acknowledgments

We thank D. Leinweber and C. Hamer for valuable conversations and suggestions. We are also grateful for access to the computing facilities of the Australian Centre for Advanced Computing and Communications (ac3) and the Australian Partnership for Advanced Computing (APAC). This work was supported by the Guangdong Provincial Ministry of Education.

---

[1] K. Bowler *et al.* [UKQCD Collaboration], Phys. Rev. D **62**, 054506 (2000)  
[2] S. Aoki *et al.* [Pc-PACS Collaboration], Phys. Rev. Lett **84**, 238 (2000)  
[3] C.J. Morningstar and M.J. Peardon, Phys. Rev. D **60**, 034509 (1999); Phys. Rev. D **56**, 4043 (1997).  
[4] A. Vaccarino and D. Weingarten, Phys. Rev. D **60**, 114501 (1999).  
[5] M. Teper, Phys. Lett. B **397**, 223 (1997); Phys. Rev. D **59**, 014512 (1998).  
[6] N.H. Shakespeare and H.D. Trottier, Phys. Rev. D **59**, 014502 (1999).  
[7] UKQCD Collaboration, G. Bali *et al.*, Phys. Lett. B **309**, 378 (1993).  
[8] J. Sexton, A. Vaccarino, and D. Weingarten, Phys. Rev. Lett. **75**, 4563 (1995), and references therein.  
[9] K. Seth, Nucl. Phys. **A675**, 25c (2000), and reference therein.  
[10] P. de Forcrand and K-F Liu, Phys. Rev. Lett. **69**, 245 (1992).  
[11] T. DeGrand, Phys. Rev. D **36**, 182 (1987).  
[12] K. Ishikawa *et al.*, Nucl. Phys. **B227**, 221 (1983).  
[13] N. Ishii, H. Suganuma, and H. Matsufuru, Phys. Rev. D **66**, 094506 (2002).  
[14] M. Loan and Y. Ying, hep-lat/0603016, submitted to Prog. Theor. Phys.

- [15] M. Albanese *et al.*, Phys. Lett. B **192**, 163 (1987)
- [16] T. Takahashi, H. Matsufuru, Y. Nemoto, and H. Suganuma, Phys. Rev. Lett. **86**, 18 (2001)
- [17] B. Velikson and D. Weingarten, Nucl. Phys. **B249**, 433 (1985)